clean technologies

Article

Development and Analysis of a Global Floating Wind Levelised Cost of Energy Map

Sergi Vilajuana Llorente *, José Ignacio Rapha and José Luis Domínguez-García

Power Systems Group, Catalonia Institute for Energy Research (IREC), Jardins de les Dones de Negre 1, 2a, Sant Adrià de Besòs, 08930 Barcelona, Spain; jirapha@irec.cat (J.I.R.); jldominguez@irec.cat (J.L.D.-G.)
* Correspondence: svilajuana@irec.cat

Abstract: Floating offshore wind (FOW) is rapidly gaining interest due to its large potential. In this regard, it is of special interest to determine the best locations for its installation. One of the main aspects when evaluating the feasibility of a project is the levelised cost of energy (LCOE), but there are many variables to consider when calculating it for FOW, and plenty of them are hard to find when the scope is all the suitable areas worldwide. This paper presents the calculation and analysis of the global LCOE with particular focus on the best countries and territories from an economic point of view, considering four types of platforms: semi-submersible, barge, spar, and tension leg platform (TLP). The model takes into account, on the one hand, wind data, average significant wave height, and distance to shore for an accurate calculation of delivered energy to the onshore substation and, on the other hand, bathymetry, distances, and existing data from projects to find appropriate functions for each cost with regression models (e.g., manufacturing, installation, operation and maintenance (O&M), and decommissioning costs). Its results can be used to assess the potential areas around the world and identify the countries and territories with the greatest opportunities regarding FOW. The lowest LCOE values, i.e., the optimal results, correspond to areas where wind resources are more abundant and the main variables of the site affecting the costs (water depth, average significant wave height, distance to shore, and distance to port) are as low as possible. These areas include the border between Venezuela and Colombia, the Canary Islands, Peru, the border between Western Sahara and Mauritania, Egypt, and the southernmost part of Argentina, with LCOEs around 90 €/MWh. Moreover, there are many areas in the range of 100–130 €/MWh.

Keywords: offshore wind energy; floating wind energy; levelised cost of energy (LCOE); cost assessment; geospatial analysis

Citation: Vilajuana Llorente, S.; Rapha, J.I.; Domínguez-García, J.L. Development and Analysis of a Global Floating Wind Levelised Cost of Energy Map. *Clean Technol.* **2024**, *6*, 1142–1168. https://doi.org/10.3390/cleantechnol6030056

Academic Editor: Shunde Yin

Received: 5 June 2024
Revised: 2 August 2024
Accepted: 27 August 2024
Published: 5 September 2024

1. Introduction

The global temperature has already risen 1.1 °C above the pre-industrial level. In 2020, concentrations of global greenhouse gases (GHGs) reached new highs. The years from 2015 to 2021 were the seven warmest on record. Because of that, GHGs must decline by 43% by 2030 according to the 2030 Agenda for Sustainable Development and to net zero by 2050. This is an almost impossible challenge that will undoubtedly require clean energy [1].

In terms of clean energies, wind has the highest potential, along with photovoltaic solar. Globally, 77.6 GW of new wind power capacity was connected to power grids in 2022, bringing the total installed capacity to 906 GW, a year-on-year growth of 9%, to which the onshore wind market added 68.8 GW while offshore wind added 8.8 GW, bringing the total global offshore wind capacity to 64.3 GW [2].

Wind is an increasingly stable form of power supply. New onshore wind farms now operate at 30–45% capacity factors and new offshore wind farms (OWF) at more than 50% [3]. This is one of the reasons why offshore wind is an interesting alternative compared to onshore wind. Furthermore, it presents other benefits, e.g., larger turbines that already reach 15–20 MW and fewer restrictions regarding land use, visual impact, and noise, and it is already a technology on a significant development path [4]. However, most of today's OWFs use bottom-fixed foundations that limit their feasible application to shallow waters [5]. It is estimated that 80% of the world's offshore wind resources are located in waters with depth greater than 60 metres (m), where traditional bottom-fixed offshore wind installations are not economically attractive or technically feasible [6]. At more than 60 m depth, only floating offshore wind (FOW) is suitable for installation. There are many locations where the waters begin to be very deep nearshore, e.g., the Mediterranean Sea, where the wind resources are some areas is high, but the development of bottom-fixed technology is unfeasible. Furthermore, to be able to install an OWF, at least a distance of 8–10 km to the shore is needed due to maritime transit, landscape pollution, etc., which makes the installation of bottom-fixed OWFs impossible nearshore [7]. The most differentiated component of FOW compared to bottom-fixed is the floating substructure, for which there are currently many prototypes being developed around the world, competing to gain a foothold in the market.

Although, as commented above, FOW technology is a suitable option for deep waters, there are other technologies that may also be good options. Ocean energy is among the renewable energies with the greatest potential for development [8]. Kinetic and potential energy are the most extractable sources produced from different ocean processes, such as waves and tides. During the period from 2003 to 2021, about 8000 papers were published on wave/tidal energy [9]; therefore, both are already studied technologies. Furthermore, due to the problem of finding sufficient space to install more PV panels, the development of photovoltaic systems in water bodies is currently attracting attention [10], which may suggest another competitor for suitable offshore space. The levelised cost of energy (LCOE) is widely used to compare the costs of different electricity generation technologies [11] and thus helps to determine the technologies that best fit each situation.

The LCOE related to FOW is currently unclear due to the immature status of the technology; there are few projects in operation and few real data, and it heavily depends on the different site conditions. However, to obtain an idea of its current situation, a market and forecast report by the QFEW Analyses Team informs about future and present offshore wind projects. One of the analyses compares the LCOE from 279 fixed and 100 FOW projects, both past and future, between 2019 and 2035. The trend line shows that the LCOEs will decrease up to about $60/MWh. Currently, there are projects in operation in Europe, e.g., the WindFloat Atlantic Pre-Commercial of 25 MW at an LCOE of $112.3/MWh [12]. Another piece of data from this report is the global under-development projects list, e.g., KF Wind Ph I or Gray Whale, both in the Republic of Korea, which stand out for their nominal power of 504 MW and 500 MW, respectively. The analysis also shows another list of planned project details, e.g., Sardegna Sud Occidentale and Hannibal, both in Italy, with nominal power of 504 MW and 250 MW, respectively [12].

Furthermore, many FOW assessments have been conducted in recent years, mainly focusing on cost assessments or site selection. Most of them are about specific territories [7,13–18], and others about specific sites [5,19,20]. In this paper, the assessment of LCOE is global.

In Diaz et al. [13], the main objective is to find a method to determine all feasible areas for floating wind energy considering technological limitations, protected and heritage zones, military areas, navigation routes, oil and gas concessions, EEZ, underwater lines and pipelines, fisheries, aquaculture, offshore marine energy locations, etc., with specific reference to Portugal, Spain, and France.

Castro-Santos et al. [14] analysed the economic feasibility of FOWFs taking into account the net present value, internal rate of return, discounted pay-back period, LCOE and cost-of-power ratio on the Galician coast in the north-west of Spain. It discards all projects that are not economically profitable with a theoretical electricity tariff of 190.856 €/MWh.

Martinez et al. [7,15] calculated and evaluated the LCOE in two studies, one for the European Atlantic and the other for the Mediterranean Sea, with a similar aim to this paper, in this case in global terms. Lerch et al. [19] delves into greater detail, focusing on three sites and comparing three types of substructures: semi-submergible concrete, tension leg platform (TLP) steel, and spar concrete.

Schallenberg-Rodríguez et al. [18] developed spatial planning to estimate the offshore wind energy potential in the Canary Islands based on a GIS that considers technical, economic, and spatial constraints.

In Bosh et al. [21], the aim is to provide a global LCOE for offshore wind energy (floating and bottom-fixed) within the EEZ. It uses the optimal technology between monopile, jacket, and tension leg buoy (TLB) depending on water depth. As a result, it presents an assessment of the cost–supply curves for the wind resources of several countries, a comparison to other studies, an analysis of the main input parameters, an evaluation of the effects of the variability of each variable, and an assessment of cost reduction potentials.

Due to the continuous development of studies and projects, the known potential, and the still-premature situation of the technology, the motivation for the realisation of this study arises. The main goal of the paper is to provide a global LCOE map that can be used as a tool to visualise and determine the best areas to place a floating offshore wind farm (FOWF) and to identify the countries with the greatest opportunities for the implementation and commercialisation of this technology, considering not only the wind resources but also the life cycle costs. Furthermore, the results can be used for a first analysis if it comes to comparing the LCOE with other technologies at specific sites. In this regard, it is necessary to develop a methodology to estimate the LCOE for all feasible areas for the technology located within the economic exclusive zone (EEZ).

All the aforementioned studies, which aim to estimate the LCOE, implement a similar methodology of four main steps. First, a search for needed geospatial data is carried out, and then the areas are filtered according to selected criteria using a geographic tool that works with cells of a certain size. If a cell or part of a cell fails to meet one of the criteria, it is eliminated for further calculations. The third step is to calculate the energy production of the remaining cells using wind speeds, capacity factor layers, and/or the power curve of the turbine being worked with. Finally, a methodology is used to calculate all the costs associated with the life cycle of the FOWF based on the distance to port, distance to shore, and water depth. The applied methodology follows the guidelines mentioned above, in this case using regression models for the cost functions. Moreover, since the variation in the LCOE as a function of different variables and life-stage costs of the FOWF is commonly analysed in the literature, a sensitivity analysis is also performed and briefly compared to the overall results of other studies.

The paper is organised into five section. The first and current section is an introduction to the technology, its necessity due to the current situation, the current state of the art dealing with the aspects of this topic, and an explanation of the aims of the study. The second chapter explains the methodology used for the development of the global LCOE map, the achieved or used functions, and the results plotted on a world map. The final two chapters present the analysis of the results and conclude the study.

2. Methodology

The development corresponds to a geographic information system (GIS) model that allows for computing the LCOE for all feasible areas worldwide. The calculations are performed with a MATLAB R2022b code for a grid of cells of 1 arc minute resolution, which is approximately equivalent to an average of 2.72 square kilometres (km^2) per cell. Calculations are divided into two parts: life cycle costs that are computed with cost functions achieved by regression models with the site conditions (i.e., distance to shore, distance to port, water depth, and average significant wave height) and costs of current projects that work with semi-submergible, TLP, barge, or spar as predictor values. The model takes the site conditions as the independent variables and the costs as the dependent variables. The second part of the calculations is the annual energy production (AEP), which in this case corresponds to the electricity delivered to the onshore substation and considers not only the wind resources of the site but also the distance to shore and the weather conditions. Furthermore, different efficiencies during the generation and transmission of energy are considered.

The *LCOE* is widely used to compare the cost of different electricity generation technologies. It is understood as the theoretical price at which the electricity would have to be sold to reach the break-even point [11]. It is also a fundamental parameter when analysing the economic viability of an energy project. In general, *LCOE* is calculated by the life cycle costs of the system (in $) divided by the lifetime electricity provided (in kWh), as shown in Equation (1) [19]:

$$LCOE = \frac{CAPEX_0 + \sum_{t=1}^{n} \frac{OPEX_t}{(1+r)^t} + \frac{DECEX_{n+1}}{(1+r)^{n+1}}}{\sum_{t=1}^{n} \frac{AEP_t}{(1+r)^t}} \quad (1)$$

where *CAPEX* is the capital expenditure, which includes costs related to the development phase, manufacturing, and installation; *OPEX* is the operational expenditure; *DECEX* is the decommissioning expenditure; *AEP* is the annual energy production; r is the discount rate; and n is the lifetime of the FOWF. The aim is to apply this function for all cells. In subsequent sections, the methodology to achieve all the information needed to apply this function is explained.

2.1. Assumptions

The LCOE is computed for the FOWF in this study; it has 20 IEA 15 MW reference wind turbines [22], which is equivalent to a total power capacity of 300 MW. The wind turbine has a hub height of 135 m. The lifetime is set to 25 years, and the discount rate (r) is set to 10% [23], as it typically has a value between 8% and 12% for offshore wind investments [24]. The life cycle costs are calculated in euros (€) with reference to 2022. Furthermore, a separation between turbines of 7 times the diameter horizontally and 7 times the diameter vertically is considered. The study attempts to estimate the LCOE of this FOWF for all feasible cells worldwide.

2.2. Data Collection

The results of the model depend largely on the quality of the data collection. Hence, an exhaustive search was conducted for the data that best fit the necessities of the study. These data can be divided into two parts: the geospatial data that determine various constraints to avoid showing unfeasible locations and are necessary for the different calculations and the project data, which are the predictor values for the regression models.

2.2.1. Geospatial Data

The geospatial data are needed to describe each cell on the world map. The data and source for each layer that is used in this work are mentioned in Table 1.

Table 1. Data layers and their corresponding data sources.

Data	Source
Bathymetry	GEBCO [25]
Significant wave height	Copernicus [26]
Wind speed at 100 m	Global Wind Atlas [27]
Wind speed at 150 m	Global Wind Atlas
Capacity factor—IEC class I	Global Wind Atlas
Capacity factor—IEC class II	Global Wind Atlas
Capacity factor—IEC class III	Global Wind Atlas
Exclusive economic zone	Marineregions [28]
Ports	Maritime safety information and AmeriGEOSS [29,30]

The significant wave height data are 12 min time series from 2011 to 2020 from the Global Ocean Waves Reanalysis provided in Copernicus. However, the needed information is the average significant wave height; hence, the calculation of the average value for each cell is conducted.

For the average wind speeds, the available layers of the Global Wind Atlas are at heights of 10, 50, 100, 150, and 200 m, but the information needed is the average wind speed at 135 m, the hub height of the wind turbine being evaluated. This is achieved by the interpolation of the average wind speed data at an elevation of 100 and 150 m.

Regarding the two port databases, a homogenisation is conducted. The first step is to relate the ports with the same names and codes, and the second step is to relate the remaining ports between the two databases that are located within 5 km of each other. Furthermore, the size of the ports is taken into account. Considering the study for medium-term installations and therefore port adaptations to the necessities of the FOWF, small, medium, and large ports are considered capable of developing installation, operation and maintenance (O&M), and dismantling activities, whereas very small ports are considered only for O&M activities. The remaining ports, the size of which is unknown, are not contemplated in any activity during the life cycle of the FOWF. It must be noted that although the costs of these three activities will increase in areas where there are no ports with the aforementioned characteristics close to the installation site, the costs of port adaptations are not contemplated.

Furthermore, the data layers must be processed to achieve homogenisation and be able to work with them at the same resolution, i.e., all layers have to be of the same size. Hence, different buffers must be applied with the QGIS' warp tool. The resulting layers have a resolution of 1 arc minute, which gives a series of cells in a 21,600 × 7800 frame.

2.2.2. Cases Data

The cost functions require an evaluation of existing cases. The evaluation is conducted with regression models working with data from various projects. Unfortunately, due to the premature situation of the technology, the existing projects are few. These projects include LIFE50+, which aims to optimise and reduce production, installation, and O&M costs for substructures designed for 10 MW turbines [23]. It develops an analysis for four different substructure concepts at three different locations. Furthermore, COREWIND is a European project providing cost-effective solutions for FOW technology [31]. In this case, the design is carried out for two substructure models (ACTIVEFLOAT and WindCrete) in three different locations. And Carbon Trust, which in a market and technology review about FOW, presents cost values submitted by concept designers with specific site conditions [32]. Furthermore, the data of Shayan Heidari [33] are used. This is a master's thesis that aims to develop an economic model for FOW that allows for calculating the total costs of a planned wind farm for three floating concepts: spar, semi-submersible, and TLP. The data obtained have cases with costs for four types of substructures: semi-submersible, barge, spar, and TLP. The analysed projects are shown in Table 2.

Table 2. Cases data and their corresponding projects or thesis.

Case	Project/Thesis
Golfe de Fos *	LIFE50+
Gulf of Maine *	LIFE50+
West of Barra *	LIFE50+
Barra **	COREWIND
Gran Canaria **	COREWIND
Morro Bay **	COREWIND
Commercial TLP	Carbon Trust
Commercial spar	Carbon Trust
Commercial semi-submersible	Carbon Trust
Spar	Shayan Heidari
Semi-submersible	Shayan Heidari
TLP	Shayan Heidari

* Costs for semi-submersible, barge, spar, and TLP cases. ** Costs for semi-submersible and spar cases.

It is also necessary to homogenise the different costs, converting each of them into costs per installed megawatt in order to conduct a correct comparison between cases.

2.3. Exclusion Areas

There are different circumstances that make the development of this technology unfeasible. Three restrictions are implemented in the model depending on the site conditions, the functionality of the technology itself, or the scope of the study, which are shown in Table 3.

Table 3. Restrictions of site conditions.

Site Condition	Restriction
Water depth	60–1000 m
Average significant wave height	<3 m
Distance to shore	EEZ

Water depth is limited because of the feasible conditions of the technology; average significant wave height is a condition to ensure suitable weather windows for installation and O&M [34]; and the EEZ is implemented as a restriction of distance to shore; all areas that are not within this zone are not contemplated. These are the ocean zones extending up to 200 nautical miles (370 km) immediately offshore from a country's coastline [35]. Moreover, although there are countries where a minimum distance to shore is established to avoid visual impact and noise nuisance, e.g., Greek territorial waters that present severe restrictions and have a minimum set of 11 km from shore, and Spain, where the restriction for offshore energy is at least 8 km away from the coast [7], still, in this work a minimum distance to shore is not established. However, a web map, which will be mentioned later in Section 3.1, allows for three different lines to be displayed at distances of 10, 20, and 30 km from the coast in case one does not wish to consider the results within these ranges. Exclusion sites such as fishing areas, maritime transit, or natural reserves are not considered either.

2.4. Annual Energy Production

The method for calculating the AEP uses different data layers from the Global Wind Atlas and the efficiency of different processes during generation and transmission to consider the AEP as the annual energy injected into the grid. Specifically, the calculation is divided into three steps:

1. Selecting the capacity factor for each cell of the world map. The Global Wind Atlas provides layers with estimated capacity factors for International Electrotechnical Commission (IEC) class I–III turbines for each grid cell. The IEC classes are standardised in IEC 61400 and describe the requirements to ensure that wind turbines are appropriately engineered against damage from hazards within the planned lifetime [36]. Therefore, wind turbine classes determine which turbine is suitable for the normal wind conditions of a particular site and are specifically determined by three parameters: average wind speed, extreme 50-year gust, and wind turbulence. However, the consideration of this study is to select the capacity factor from the different IEC class layers depending only on the average wind speeds at 135 m. The capacity factor will be the value given in IEC class III when average wind speeds are below 7.5 m/s and will be determined by the interpolation of the IEC III and II capacity factors for average wind speeds between 7.5 and 8.75 m/s, the interpolation of the IEC II and I capacity factors between 8.75 and 10 m/s, and the IEC class I value for average wind speeds above 10 m/s. This can be made clearer by Table 4. The interpolations are applied to smooth out the decrease or increase in capacity factor at locations where average wind speeds change to just above 7.5 m/s or just below 10 m/s. And no maximum average wind speed is considered so as not to eliminate cells due to this variable.

2. Calculating the ideal AEP per MW with the capacity factors resulting from point 1, as shown in the following equation.

$$IdealAEP(x,y) = CF(x,y) \cdot 1\text{ year} \cdot 365.25\frac{\text{days}}{\text{year}} \cdot 24\frac{\text{h}}{\text{day}} \cdot 1\text{MW} \tag{2}$$

3. Applying different factors that affect the efficiency of generation and transmission to the onshore substation. Although the losses can vary significantly depending on each case, e.g., array losses can vary with the performance of the FOWF or cable length, and wake losses can change due to the distances between turbines or wind conditions, they are considered constant. The wake efficiency is set at 93%, and the array efficiency is set at 99% [33]. Substation efficiency is also considered and is set to 98%. Furthermore, the export cable efficiency and availability are computed depending on distance to the onshore substation and average wave height, respectively, as shown in Equations (3) and (4):

$$ExportEff(x,y) = \frac{99 - DistONS(x,y) \cdot k}{100} \tag{3}$$

$$Availability(x,y) = \frac{98 - SWH(x,y)^3}{100} \tag{4}$$

where *DistONS* is the distance to the onshore substation, in this case, the distance to shore; *k* is the rate of decrease in efficiency per distance unit set at 0.02; and *SWH* is the average significant wave height at coordinates (*x*,*y*), which is used to characterise the weather conditions.

Table 4. Capacity factor selected depending on average wind speed.

Average Wind Speed at 135 m	Capacity Factor
WS $\leq$ 7.5 m/s	IEC class III
7.5 m/s < WS $\leq$ 8.75 m/s	Interpolation IEC class III and II
8.75 m/s < WS $\leq$ 10 m/s	Interpolation IEC class II and I
WS > 10 m/s	IEC class I

2.5. Life Cycle Costs

In this study, the life cycle costs depend on three different variables: distance to port, distance to shore, and water depth. As mentioned above, the functions are based on regression models, and in order to make the functions more accurate, these costs are separated into development costs, mooring system costs, turbine costs, substructure costs, electrical system costs, installation costs, operation expenditure (OPEX), and decommissioning expenditure (DECEX).

The cost functions are computed from the data of the existing projects mentioned above in Table 2. Each case has its own variables of distance to shore, distance to port, and water depth. With these databases for the cost values and the help of the Excel data analyser tool and RStudio, the regressions can be executed. Each regression has the values of the variables mentioned above as independent variables and the value of stage cost (in this case, per MW) as the dependent variable. Depending on the quality of the coefficients obtained, evaluated by their *p*-values, and the known relationship between independent and dependent variables based on their practical significance and the comments in the literature, it is determined which are more accurate to contemplate for each of the cost functions. The resulting functions are explained below.

The mooring system involves the anchors and mooring lines and is in charge of keeping the wind turbine on site [37]. Its type, load, and length have an effect on the costs, but in this case only the water depth is considered:

$$Mooring\ system\ costs\ (x,y) = C1 + C2 \cdot depth(x,y) \tag{5}$$

where *C*1 and *C*2 are the coefficients given by the regression, and *depth* is the water depth at coordinates (*x*,*y*).

The substructure is the component responsible for keeping the turbine afloat, and its design must ensure needs such as stability in intact conditions, safety for personnel and the environment, and adequate fatigue resistance for 20–30 years [38]. However, as this study aims to find an average of the costs for the four substructure types, and no significant variance in substructure costs has been observed with respect to any of the variables, an average of the costs of the different projects is used, approximately 0.95 M€/MW.

The turbine costs cover all wind turbine components and the tower. The value used is the average of the data collection values. The result is approximately 1.5 M€/MW, similar to the values found in the literature.

The electrical system involves the inter-array system, the offshore substation, and the export cables. These are the components for the transmission of the electricity generated from the wind turbines to the shore [39]. In this case, the distance to the onshore substation, which is considered the distance to shore, and the water depth are the variables affecting the cost calculations:

$$Electrical\ system\ costs\ (x,y) = C1 + C2 \cdot DistONS(x,y) + C3 \cdot depth(x,y) \tag{6}$$

where *C*1, *C*2, and *C*3 are the coefficients given by the regression; *DistONS* is the distance to shore; and *depth* is the water depth at coordinates *(x,y)*.

Installation is the last step before the commissioning of an FOWF. It covers the delivery of all components to the onshore assembly site, the assembly itself, the transport to the installation site, and the installation offshore [40]. Although installation costs depend on many variables, in this case, as seen in Equation (7), only the distance to port affects the result:

$$Installation\ costs\ (x,y) = C1 + C2 \cdot DistPort1(x,y) \tag{7}$$

where *DistPort*1 is the distance to the closest port with installation capabilities according to this study.

Development costs, which include all activities related to the initial development design of the FOWF up to the point at which the official orders for production and purchasing are made, are calculated as follows:

$$Development\ costs\ (x,y) = CAPEX(x,y) \cdot C \tag{8}$$

where *CAPEX* is the sum of turbine, substructure, mooring system, electrical connection, and installation costs for its respective coordinates and *C* is a 5.7% factor considered [41].

The OPEX encompasses the O&M activities consisting of scheduled and unscheduled maintenance and the manufacturing of replaced components during the entire lifetime of the FOWF:

$$OPEX(x,y) = C1 + C2 \cdot DistPort2(x,y) \tag{9}$$

where *DistPort2* is the distance to the closest port with O&M capabilities according to this study.

DECEX represents the costs occurring at the end of life incurred from the decommissioning of the FOWF. In this paper, it is considered 8% more expensive than installation costs; hence, the DECEX is computed as follows:

$$DECEX(x,y) = Installation\ costs\ (x,y) \cdot 1.08 \tag{10}$$

2.6. Regression Model Summaries

This subsection shows the summaries of the functions achieved by the regression models. As commented above, in the substructure and turbine cases, the values used are the averages. In Figure 1, there is some information about the cost functions, such as the residuals, the coefficients and their related *p*-values, the residual standard error, the multiple

R-squared, the adjusted R-squared, and the F-statistic. If the focus is on the p-values of the intercept coefficients, they are always below 0.05, for which it can be considered that the values are significant [42]. Regarding the rest of the coefficients, the p-values range from 1.49×10^{-12} to 0.548, but only the minimum p-value satisfies the condition of p-value < 0.05. Hence, only one of the independent variables can be considered statistically significant. However, knowing the difficulty of achieving high statistical quality due to the lack of data (and thus small sample size), the known relationship between independent and dependent variables, the known practical significance, and the non-negative coefficients achieved, they are considered adequate as the functions for the life cycle costs.

(a) Residuals:

Min	1Q	Median	3Q	Max
−343,422	−88,501	3792	55,713	731,728

Coefficients:

	Estimate	Std. Error	t value	Pr (>|t|)
Intercept	219,455	57,393.7	3.824	8.22×10^{-4}
Depth	353.9	218.3	1.621	0.118103

Residual standard error: 212,500 on 24 degrees of freedom
Multiple R-squared: 0.09867, Adjusted R-squared: 0.06112
F-statistic: 2.627 on 1 and 24 DF, p -value: 0.1181

(b) Residuals:

Min	1Q	Median	3Q	Max
−545,678	−231,409	−123,776	260810	884,261

Coefficients:

	Estimate	Std. Error	t value	Pr (>|t|)
Intercept	959,011	72,611	13.21	8.95×10^{-13}

Residual standard error: 370,200 on 25 degrees of freedom

(c) Residuals

Min	1Q	Median	3Q	Max
−293,310	54,563	54,563	63,265	148,176

Coefficients:

	Estimate	Std. Error	t value	Pr (>|t|)
Intercept	1,493,310	29,208	51.13	$<2 \times 10^{-16}$

Residual standard error: 148900 on 25 degrees of freedom

(d) Residuals:

Min	1Q	Median	3Q	Max
113,749	−65323	18,323	49,900	145,446

Coefficients:

	Estimate	Std. Error	t value	Pr (>|t|)
Intercept	300,748	36,712	8.192	8.06×10^{-8}
DistONS	5202.74	337.93	15.396	1.49×10^{-12}
Depth	134.55	88.36	1.523	0.143

Residual standard error: 81,280 on 20 degrees of freedom
Multiple R-squared: 0.925, Adjusted R-squared: 0.9175
F-statistic: 123.3 on 2 and 20 DF, p -value: 5.627×10^{-12}

(e) Residuals:

Min	1Q	Median	3Q	Max
−313,003	−195,162	−99,107	114459	1,347,041

Coefficients:

	Estimate	Std. Error	t value	Pr (>|t|)
Intercept	417,105	95,978	4.346	2.19×10^{-4}
DistPort1	507.9	676.3	0.751	0.459994

Residual standard error: 337,300 on 24 degrees of freedom
Multiple R-squared: 0.02296, Adjusted R-squared: −0.01775
F-statistic: 0.5639 on 1 and 24 DF, p -value: 0.46

(f) Residuals:

Min	1Q	Median	3Q	Max
−49,563	−35,239	13,733	28,296	62,740

Coefficients:

	Estimate	Std. Error	t value	Pr (>|t|)
Intercept	96,876	10,830.03	8.945	4.14×10^{-9}
DistPort2	46.46	76.31	0.609	0.548

Residual standard error: 38,060 on 24 degrees of freedom
Multiple R-squared: 0.01521, Adjusted R-squared: −0.02582
F-statistic: 0.3706 on 1 and 24 DF, p -value: 0.5484

Figure 1. Regression model summary of (**a**) mooring system costs, (**b**) substructure costs, (**c**) turbine costs, (**d**) electrical system costs, (**e**) installation costs, and (**f**) OPEX.

2.7. Levelised Cost of Energy Calculation

Once the functions are determined, they have to be applied to all feasible cells. The functions require each of the independent variables, which are obtained in different ways. The water depth is extracted directly from the bathymetry layer. The distances are computed with a MATLAB R2022b function based on the Haversine algorithm [43]. The distance to shore considers the latitudes and longitudes of the feasible cell and the nearest cell from the coast, whereas the distance to port is computed as the distance from the feasible cell to the nearest port. Furthermore, the capabilities of the ports are taken into account; hence, two different layers have been computed, one for the installation costs (Equation (7)) and the other for OPEX (Equation (9)). Finally, the average significant wave height is extracted from the average computation commented above in Section 2.2.1.

The cost functions, the AEP function, and the assumptions are applied and related as shown in the LCOE equation (Equation (1)) for each feasible square of the grid with a MATLAB R2022b code, and the results are obtained.

3. Results

The analysis of the results corresponds to the realisation of a ranking of countries and territories (which will be referred to as ranking of territories throughout the paper) with an interpretable method that helps to determine which zones have the highest potential, which in this case corresponds to the areas with the lowest LCOE values. The method considers the potential area, the average LCOE of the technology in the case that it produces 20% of the energy production of the territory, and the LCOE of the best area to locate the FOWF of the study (an FOWF with a capacity of 300 MW). In addition, two sensitivity analyses are presented in order to visualise the effects on the LCOE due to the increase or decrease in the input variables or different life cycle costs. Specifically, the following sections present a first representation of the results (Section 3.1), a histogram to see the behaviour of the values obtained (Section 3.2), a sensitivity analysis of the main variables considered for the LCOE calculations (Section 3.3), a sensitivity analysis of the life cycle costs (Section 3.4), the criteria applied before the analysis of the best territories (Section 3.5), four different ranking of territories (Section 3.6), and the LCOE map of the top 10 territories and their analyses (Section 3.7).

3.1. Representation of the LCOE Results

Using QGIS, the results can be represented with a colour scale to discover which are the most interesting areas to implement this technology. The representation of the LCOE layer is published with an interactive web map at this link: https://floatingwindmap.energysmartlab.com (accessed on 5 June 2024). It also has an explanation of the main aspects of the realisation and assessment of the results. The data represented on the web map are similar to those shown in Figure 2.

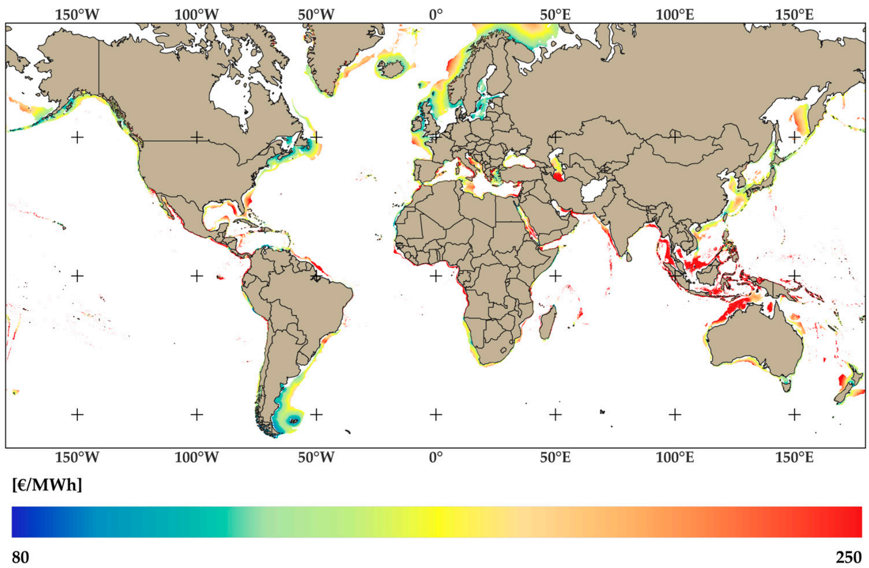

Figure 2. Global floating wind LCOE map.

3.2. Distribution of the LCOE Values

The range of values obtained goes from 80 €/MWh to 22,149 €/MWh; hence, there are values in the global LCOE map that are not economically suitable. The histogram in Figure 3 helps to analyse the number of interesting values. There is little surface where the LCOE is between 80 and 110. Even in the interval between 80 and 90 €/MWh, although the existence of values is not visible in the histogram, there are 2091 square kilometres (km^2)

with LCOE between these two values. From 120 €/MWh onwards, a great increase in the area is observed. Up to 160 €/MWh, it continues growing, which is the largest surface registered (between 150 and 160 €/MWh), with 1,596,980 km^2. From here, the surface area per interval decreases until 250 €/MWh, which is the last value recorded in the histogram. Hence, values near the maximum commented above are extreme results and rarely appear on the map.

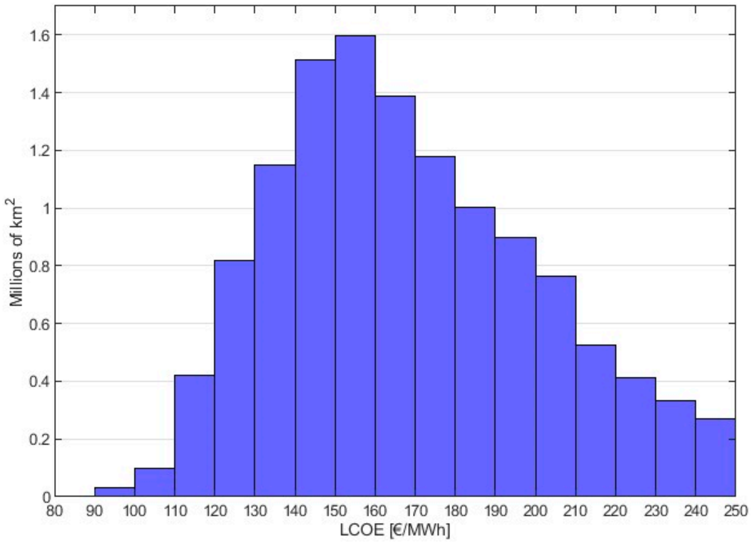

Figure 3. Amount of area with values from 80 €/MWh to 250 €/MWh, represented in intervals of 10.

3.3. Sensitivity Analysis of the Input Variables

There are seven main variables that affect the results of the LCOE: water depth, average significant wave height, capacity factor, distance to shore, distance to installation port, distance to O&M port, and discount rate. To see which have the greatest impact, the effects on the LCOE mean have been analysed when the values of each variable are increased or decreased by 25% while the rest remain constant. This is the one-factor-at-a-time method. The results are represented in Figure 4.

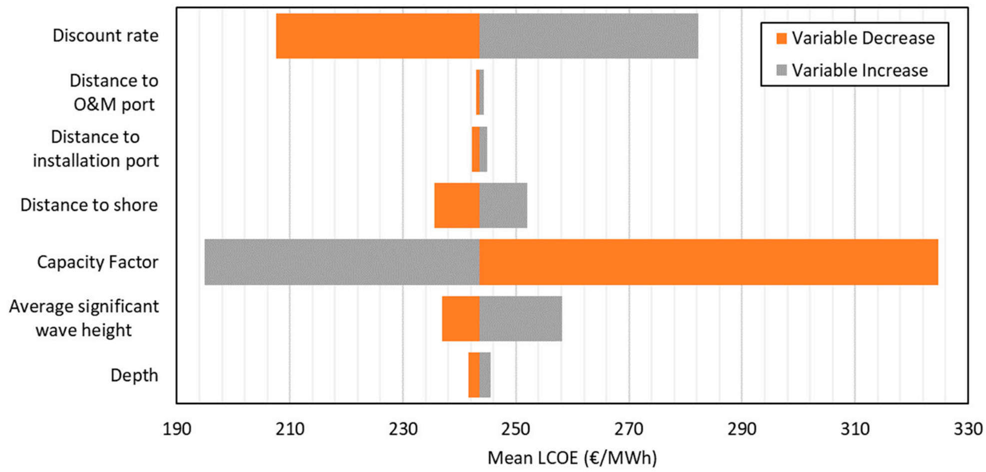

Figure 4. Assessment of the main variables affecting the LCOE mean with the one-factor-at-a-time method.

Based on the baseline average LCOE of 243.58 €/MWh obtained from the global results under normal conditions, altering the capacity factor or discount rate has the largest impacts on the LCOE. By increasing or decreasing the capacity factor by 25%, the difference obtained in the LCOE is +81.19 €/MWh or −48.72 €/MWh. This is equivalent to a relative effect of +33.33% on the LCOE mean when decreasing the capacity factor and of -20% when increasing it. Regarding the discount rate, the variability in the input argument modifies the LCOE mean with an increase of +38.69 €/MWh and a decrease of −35.99 €/MWh, a relative change that is around ±15%, a lower impact than modifying the capacity factor. The rest of the variables have lower impacts. Decreasing the average significant wave height results in a benefit of −6.72 €/MWh, which is −2.76%, and the increase transforms into +14.55 €/MWh, which is +5.97%. For distance to onshore substation, water depths, and both distances to port, the variability modifies the LCOE mean by +3.46–3.30%, ±0.82%, ±0.57%, and ±0.28%, respectively, with the variance for the O&M port being lower than for the installation port.

3.4. Sensitivity Analysis of the Life Cycle Costs

In this section, the objective is similar to that in the previous section, but this time the analysis focuses on the effect of the variance in the costs of the different life cycle stages on the LCOE. The stages correspond to each of the functions discussed in Section 2.5. These are the costs related to development, mooring system, substructure, turbine, electrical system, installation, O&M, and decommissioning. These two analyses can be used to determine potential future cost reductions for the technology and validate the model comparing these results with the obtained in other studies. The results of the analysis are shown in Figure 5.

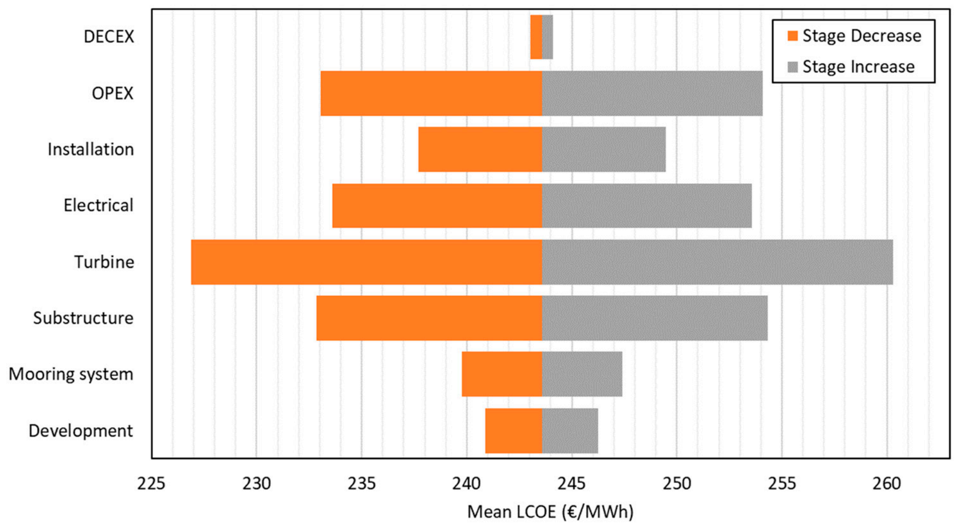

Figure 5. Assessment of the life cycle costs affecting the LCOE mean with the one-factor-at-a-time method.

The greatest impact comes from increasing and decreasing the turbine (and tower) costs by 25%. The change in the LCOE mean is ±16.72 €/MWh, which is a relative change of ±6.86%. After turbine costs, there are three stages that have a similar impact on the LCOE: substructure, OPEX, and electrical costs, which cause variances of ±10.74 (±4.41%), ±10.53 (±4.32%), and ±9.98 €/MWh (±4.10%), respectively. For the increases and decreases in the installation, mooring system, and development costs, the LCOE mean is modified by ±5.89, ±3.82, and ±2.69 €/MWh, which are still significant effects. Finally, DECEX has the lowest impact, with a variance of ±0.53 €/MWh. These variations directly show the burden of each life-stage cost; as in other studies [7,15,19], the largest burden comes from the manufacturing stage (turbine, substructure, electrical, and mooring system), followed by the O&M, the installation costs, the development, and finally the DECEX.

3.5. Criteria before the Territory Analysis

In order to decide which territories have the greatest potential to harness FOW energy, previous criteria have been applied to the results. In addition to the restrictions on the global floating wind LCOE map, there are other considerations that cause limitations for the installation of an FOWF, e.g., protected areas, heritage restriction zones, military areas, and licensed areas for hydrocarbon exploration and exploitation [44]. However, due to the difficulty of finding some of these layers for the whole world, only heritage and protected zones have been excluded for the evaluation of the results. A minimum distance to shore is also applied. Although each country has its own restrictions, for this study, it is considered 10 km. Furthermore, due to the selection of territories to be analysed, a maximum LCOE has been implemented, i.e., all areas with an LCOE higher than the established one have been eliminated.

Finally, a minimum area of remaining cells has also been established. With the above considerations applied, small areas remain, even isolated cells in some areas of the map. Therefore, a minimum area related to the area occupied by the FOWF under study is considered. This FOWF has 20 turbines; hence, the area criterion is the same as what it would occupy with a distribution of 4 × 5 turbines. The minimum area is the result of the equation below:

$$MinimumArea = (7 \cdot D \cdot 5) \cdot (7 \cdot D \cdot 4) \tag{11}$$

where D is the diameter of the rotor, 7 is the rotor diameter factor for the distance between turbines, and 5 and 4 are the number of distances between turbines plus a margin of 3.5D considered on each side.

There are several territories that have no cells in their EEZ after applying the criteria explained above and shown in Table 5. These territories are removed from the analysis, while the remaining territories are analysed and compared in the subsequent sections.

Table 5. Exclusion areas applied before the best territories analysis.

Criteria	Exclusion Areas
Protected zones [45]	All
Heritage zones [45]	All
Minimum distance to shore	10 km
Maximum LCOE	130 €/MWh
Minimum area	56.4 km^2

3.6. Analysis of Territories with LCOE < 130 €/MWh within Their EEZ

After the data filter discussed in Section 3.5, this study still has data for 56 territories. However, the evaluation continues to find the top 10 territories with a three-factor model.

3.6.1. Analysis Factors

The first factor consists of calculating the resulting area after the criteria commented in Section 3.5 for each territory, which will be considered its potential area. The second factor is the LCOE mean for the production of 20% of the 2022 electricity production of the territory [46] with the cells with the lowest values of LCOE, and the third factor is the best area to locate the FOWF of study depending only on the LCOE, i.e., the area of 56.4 km^2 where the average LCOE is the lowest for each territory. The objective is to find the result of these three factors for the 56 territories and show the top 10 for each of them.

For the second factor, it is necessary to consider a power density. Knowing the FOWF power capacity (300 MW) and its area (56.4 km^2), the division between both values gives the required parameter. This equates to a power density of 5.32 MW/km^2, which does not differ much from the offshore wind value obtained by Enevoldsen et al. 2021 [47] of 7.20 MW/km^2. With this relation and the calculation of the cell area, the power capacity per cell can be computed, and if that capacity is replaced by the value of 1 MW in Equation (2), then the energy produced by the cell is obtained. For each country, the necessary cells with the minimum LCOE are selected until reaching the 2022 production of the territory. Furthermore, these calculations consider the LCOE layers of the territory before applying the criteria of maximum LCOE and minimum area to ensure that the necessary cells to meet the established electrical production are taken into account. The resulting rankings are shown in Tables 6–8. Furthermore, the sum of the power capacity per cell to reach the set production is presented for each territory in Table 7 as the power needed for the set production.

Table 6. Top 10 territories depending on the resulting potential area.

Territory	Potential Area (km^2)
Argentina	216,234
Canada	164,356
Falkland Islands	92,492
United Kingdom	52,176
Sweden	48,953
Alaska	42,507
Russia	32,255
Western Sahara	31,695
Norway	26,438
United States	21,989

Table 7. Top 10 territories depending on the LCOE mean to set 20% of the 2022 electricity production.

Territory	LCOE Mean for the Set Electricity Production (€/MWh)	Power Needed for the Set Production (MW)
Peru	90.79	2032
Colombia	92.34	2866
Venezuela	94.05	3402
Argentina	94.25	5322
Aruba	94.76	36
Falkland Islands	97.47	11
Madagascar	101.05	89
Alaska	102.78	272
New Zealand	103.32	1733
Yemen	106.17	160

Table 8. Top 10 territories depending on the minimum LCOE for the FOWF.

Territory	Minimum LCOE for the FOWF (€/MWh)
Colombia	89.15
Peru	89.80
Venezuela	91.07
Argentina	92.41
Western Sahara	94.88
Egypt	95.09
Aruba	96.48
Falkland Islands	97.76
Vietnam	100.91
New Zealand	102.09

3.6.2. Ranking According to the Three Factors

The answer to the best territories can be ambiguous, but this study aims to use the factors computed above to determine them with a specific and interpretable method. The evaluation is conducted considering the points obtained by each territory; the more points, the better the ranking position. The scoring is out of 100 points, of which each of the factors has a weight of 33.33%.

For the score regarding the potential area obtained, the maximum value, which corresponds to that obtained by Argentina, is divided by 33.33, and the value resulting from this operation is used for the score of all the territories. The resulting area of each of them is divided by the previous result, so that the greater the potential area, the greater the resulting value between the minimum value and 33.33.

For the remaining two factors, the difference between the maximum and minimum LCOE is calculated and divided by 33.33. Next, the difference between the resulting values of each territory and the maximum is divided by the result from the prior calculation. In this case, the lower the resulting LCOE, the higher the resulting value between 0 and 33.33.

Furthermore, two restrictions have been considered. First is an evaluation of the needed power capacity to satisfy 20% of the 2022 electricity production. If a territory does not need at least 300 MW, which is the power of the wind farm in the study, the territory is excluded from the ranking. Among others, this is the case of the Falkland Islands, Aruba, Alaska, and Madagascar, with 11, 36, 272, and 89 MW, respectively. Without this restriction, the territories would reach positions 2, 7, 8, and 10. The second restriction is that if there is a territory that has no value in one of the three aspects, it is also excluded from the ranking. This is the case of Western Sahara, for which 2022 electricity production is not available, and therefore the LCOE mean analysis is not possible.

The scores obtained are added together to obtain the score out of 100. With these results, it is possible to complete the ranking (see Appendices A and B for the complete ranking). The top 10 territories and their scores are shown in Table 9.

Table 9. Top 10 territories depending on the three factors of punctuation.

Territory	Points
Argentina	95.0
Peru	68.8
Colombia	67.6
Venezuela	65.6
Canada	62.9
New Zealand	50.9
Egypt	49.0
Vietnam	47.6
United Kingdom	43.5
Chile	41.5

It must be noted that this scoring model is an approach selected for the purpose of obtaining an overview of the territories that may present the greatest likeliness for future commercialisation with FOW, in this case, from a technical–economic point of view without considering the financial or policy situation of each territory. Furthermore, this is analysed by the values of the global LCOE map with baseline assumptions, and site-specific analyses may present more accurate calculations of the LCOE.

Figure 6 helps to compare and visualise the scores of the territories for each of the factors discussed above.

Based on the results, it is proven that the previous three rankings provide clues about how the final top 10 will turn out. All territories that appear in the top 10 except Chile appear in at least one of the three previous rankings. Argentina, reaching the first position in the top 10, is the only country that achieves a position in the top 10 of all three factors. Argentina and Canada stand out in terms of their potential areas, with the highest and second highest values, respectively. Regarding the other two factors, the difference in scores is not so noticeable, since the LCOE values do not differ too much between all the territories within the top 10, and all of them reach at least position 21 in both aspects.

3.7. Detailed Results of the Top 10 Territories

In this section, the maps of the top 10 territories for FOW are presented. Specifically, the following subsections analyse each of the territories with their corresponding LCOE maps, showing only values lower than 130 €/MWh to focus on the best areas, and a provide brief review of existing studies mentioning their offshore wind potentials, with a special focus on FOW.

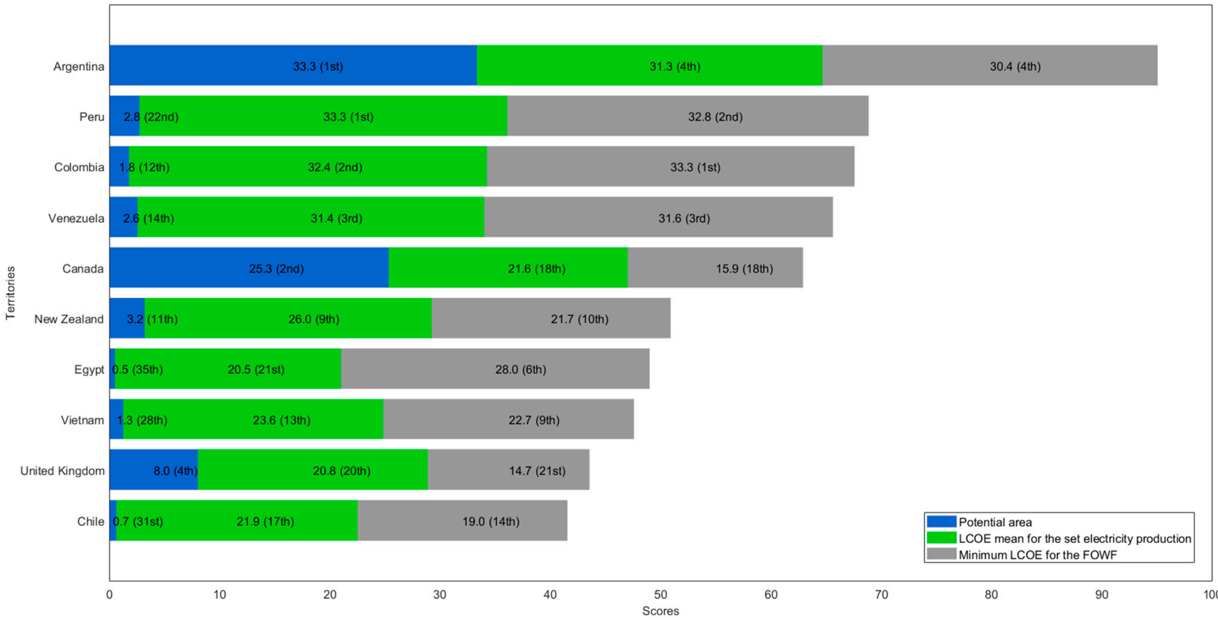

Figure 6. Top 10 territory scores and positions per factor.

3.7.1. Argentina

Argentina, which is the tenth territory with the greatest FOW potential according to The World Bank [48], has achieved the first position in this ranking. As shown in Figure 7, the best zone is in the southern part of the country, with LCOEs around 90 €/MWh. There are already published studies that analyse the potential of both wave and wind energy on the Argentine coast, focusing on Patagonia [49]. Although it corresponds to a sparsely populated zone, it is of special interest due to the possibility of generating large quantities of green hydrogen [50]. The Patagonian coasts correspond to one of the offshore areas with the highest average wind speeds registered, which in the Argentine part reach 12.5 m/s.

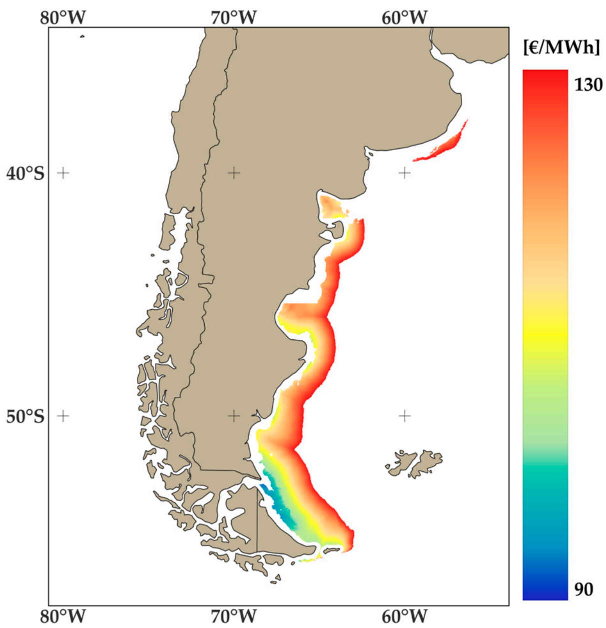

Figure 7. Argentina LCOE (<130 €/MWh) map.

3.7.2. Peru

Peru has an extensive coastline with interesting LCOE values, mainly near Independence Bay, where values slightly below 90 €/MWh are found. Although no studies have been found that analyse Peru's offshore wind resources, it is known that it has a high potential on its coasts, especially in the regions of Piura, Lambayeque, La Libertad, Ancash, Arequipa, and Ica (where Independence Bay is located), which correspond to the zones with the most cells with an LCOE below 130 €/MWh, as shown in Figure 8.

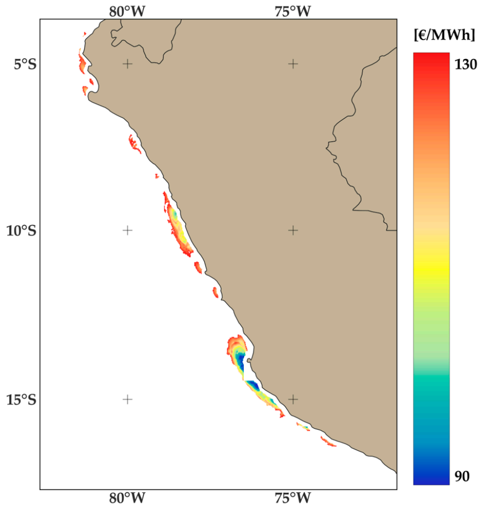

Figure 8. Peru LCOE (<130 €/MWh) map.

3.7.3. Colombia

The area of Colombia with the lowest values corresponds to the northeast part of the country, on the coasts of the department of La Guajira, as shown in Figure 9. Costoya et al. 2019 [51] and Bethel 2021 [52] analyse the wind potential of the Caribbean Sea and comment separately on the potential of Colombia, the latter highlighting the wind speeds of the La Guajira region. Other papers, such as Rueda-Bayona et al. 2019 [53], work specifically on the offshore wind potential of the Colombian coasts, which aims to justify the need for the country's research in offshore wind and also emphasises the La Guajira region. Furthermore, Colombia is the first country in the top 10 that appears in the ranking of the 30 main markets of the Floating Offshore Wind—A Global Opportunity report [54], which considers seven parameters related to the competitiveness and policy environment of FOW markets.

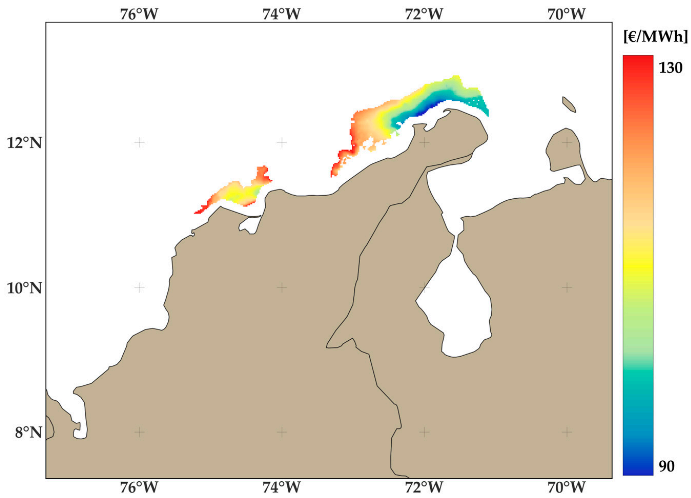

Figure 9. Colombia LCOE (<130 €/MWh) map.

3.7.4. Venezuela

Venezuela, bordering Colombia, belongs to one of the best zones obtained in this paper, the northernmost part of South America. Venezuelan waters are also located in the Caribbean Sea, which is analysed in the papers commented in the previous subsection. The best cells in this zone, which are shown in Figure 10, have average wind speeds ranging from 10 to 11.25 m/s, resulting in capacity factors around 60%.

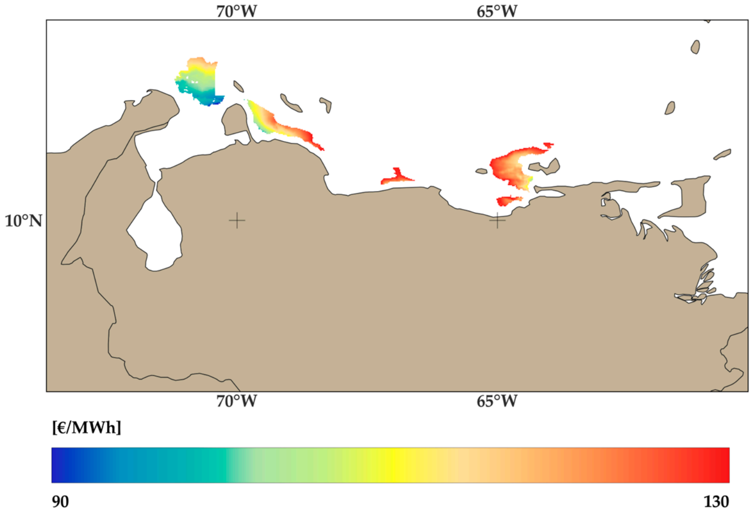

Figure 10. Venezuela LCOE (<130 €/MWh) map.

3.7.5. Canada

As in The World Bank study [48], Canada has the second-greatest potential for FOW. Furthermore, it is the eighth country best positioned in the Floating Offshore Wind—A Global Opportunity report [54] ranking. In Dong et al. 2021 [55], the offshore power potential of Canada is investigated, and it is concluded that the gross power potential of its offshore surface is thirty times the electricity production of the country in 2019.

Almost all of Canada's potential is located on the east coast; the best results and the largest potential areas for this country are found there, as shown in Figure 11.

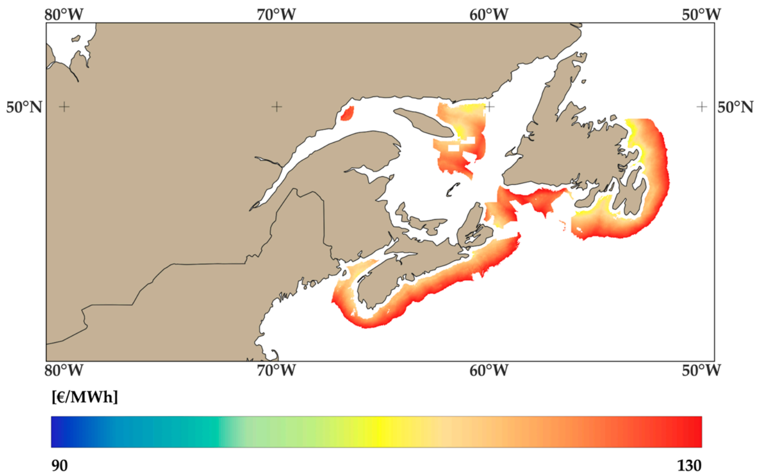

Figure 11. Canada east coast LCOE (<130 €/MWh) map.

However, there is a considerable potential area on the westernmost coast of Canada, in the province of British Columbia, as seen in Figure 12.

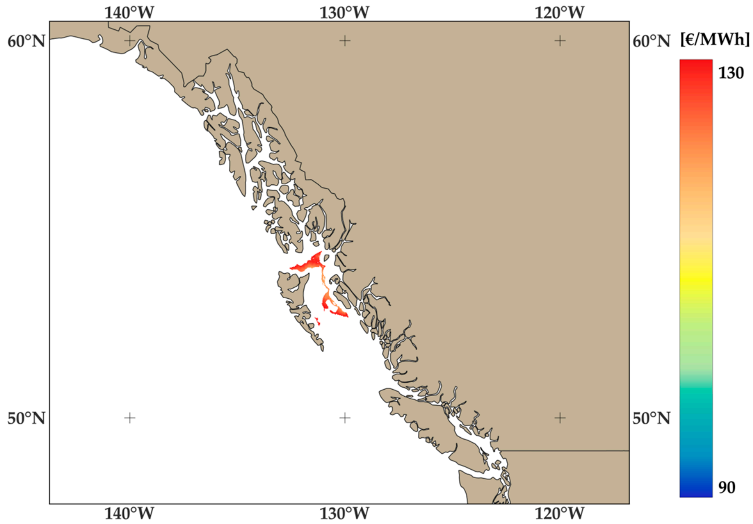

Figure 12. Canada west coast LCOE (<130 €/MWh) map.

3.7.6. New Zealand

New Zealand's best results are between the North and South Islands, which can pose a problem because this area corresponds to a high maritime density zone, which can be a limitation for FOWFs. Furthermore, New Zealand has a large potential zone located on the south coast and three other zones around the North Island. There is a study that aims to calculate the expected values of energy and classify the different offshore areas of the country with a micro-scale classification of offshore wind energy sources [56]. It concludes that all nearshore zones are considered rich areas, but it emphasises the North Cape waters, the East Cape waters, the South Taranaki Bight, the northwest waters, and a wide range in the south of the Stewart Island. In Figure 13, there is a small area in the East Cape waters, the greatest area near to South Taranaki Bight, which is the area mentioned previously between the North and South Islands, and another considerably large area near Stewart Island.

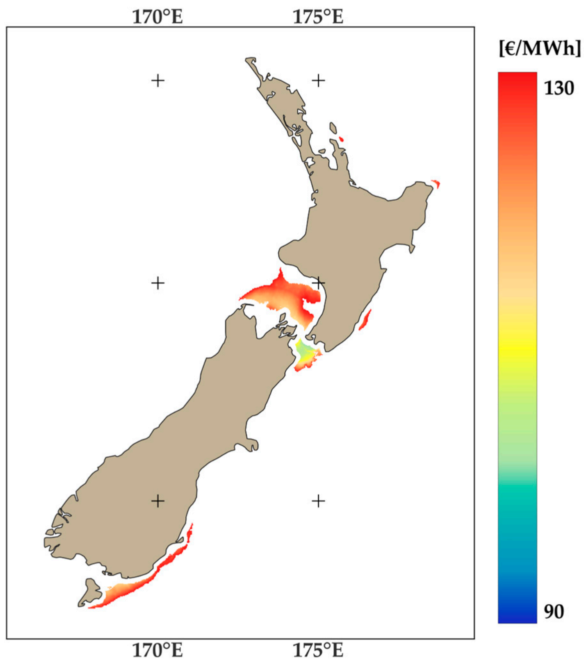

Figure 13. New Zealand LCOE (<130 €/MWh) map.

3.7.7. Egypt

Egypt is also mentioned in the Floating Offshore Wind—A Global Opportunity report [54], reaching the twenty-fourth position in the ranking. Furthermore, there is a paper dedicated to its offshore wind potential, Mahdy et al. 2018 [57], which presents a spatial analysis and highlights three areas that mainly contain suitability conditions for bottom-fixed offshore wind farms. One of these areas is located in Saudi Arabian waters, and the remaining two are located in Egyptian waters, which are close to the two smallest areas that appear in Figure 14, in this case for FOW.

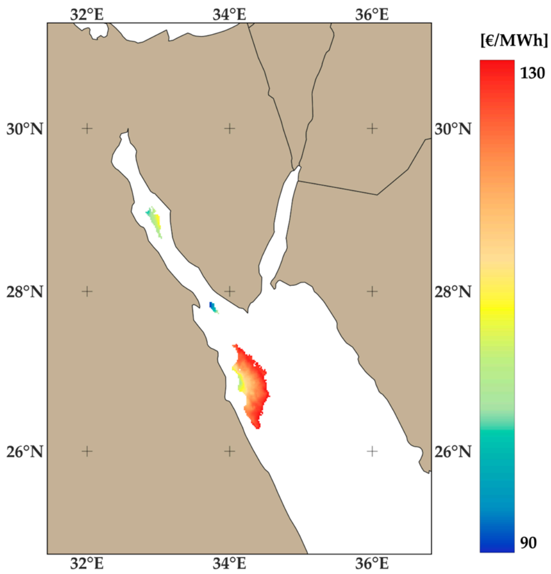

Figure 14. Egypt LCOE (<130 €/MWh) map.

3.7.8. Vietnam

Vietnam only has values below 130 €/MWh in an area near Phan Rang, as shown in Figure 15. This territory also appears in the Floating Offshore Wind—A Global Opportunity report [54] and is one of the most prominent countries, commenting on the possibility of introducing this technology in the targets of the country and the relationship that it may have with the production of green hydrogen.

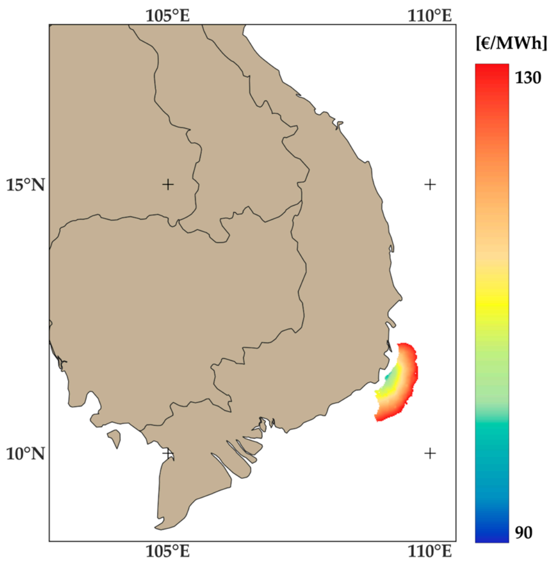

Figure 15. Vietnam LCOE (<130 €/MWh) map.

3.7.9. United Kingdom

The United Kingdom is the leading territory for offshore wind energy, but almost all its projects are installed with bottom-fixed technology due to its large areas with shallow water and high wind potential. However, it also has a large potential for FOW energy, and has the first full-scale FOWF (the Hywind Scotland) and the second-largest FOWF to date, named Kincardine, 16 km off the coast of Aberdeen, which has five 9.5 MW wind turbines. Almost all of its coast has potential areas, as shown in Figure 16, but the most interesting values are located between the island of the United Kingdom and island of Ireland, reaching values around 110 €/MWh. However, as in the case of New Zealand, this zone is a strait with high maritime density, which can be a limitation for FOWFs. There are studies that analyse the United Kingdom's offshore wind potential but involve both bottom-fixed and FOW from an economic point of view, mapping the LCOE, e.g., Cavazzi et al., 2016 [58], and Bosch et al., 2019 [21]. They present the LCOE for deep and shallow waters. The range of values achieved by the Cavazzi et al., 2016 [58], LCOE map is similar to the results of this study. Furthermore, it is the only country in the top 10 that is considered a mature floating market by the Floating Offshore Wind—A Global Opportunity report [54].

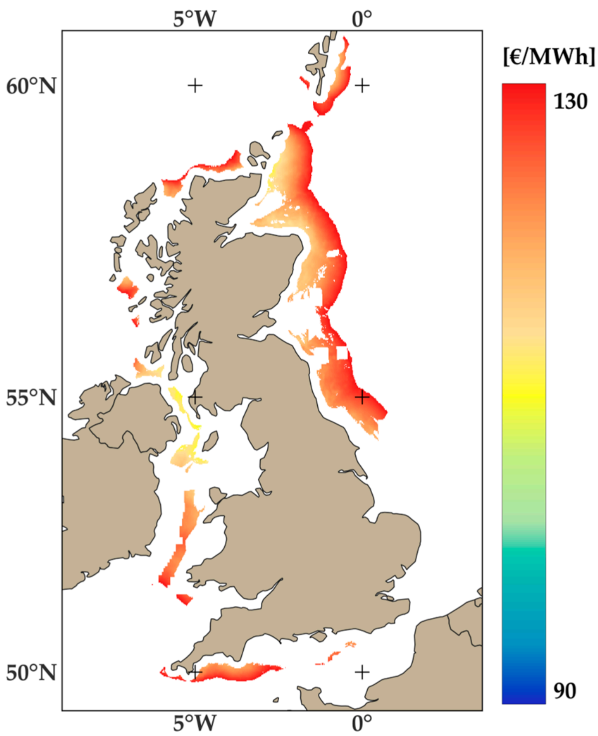

Figure 16. United Kingdom LCOE (<130 €/MWh) map.

3.7.10. Chile

The lowest Chilean results are located on the southern coast, as seen in Figure 17, near Tierra del Fuego, which, as commented above, is a sparsely populated zone but may be of interest for green hydrogen production. In the Floating Offshore Wind—A Global Opportunity report [54], Chile reaches the twenty-first position of the ranking, and the report specifies that the country has a plan in preparation for hydrogen. Furthermore, the most recent research article on the potential of offshore wind energy in Chile, Mattar et al., 2021 [59], which aims to break the paradigm of offshore wind in Chile and bases its estimations for a 608 MW offshore wind project located along the Chilean coast, concludes that Chile has large areas that can be competitive in terms of offshore wind technologies; specifically, it presents that 80% of the studied area contains favourable sites.

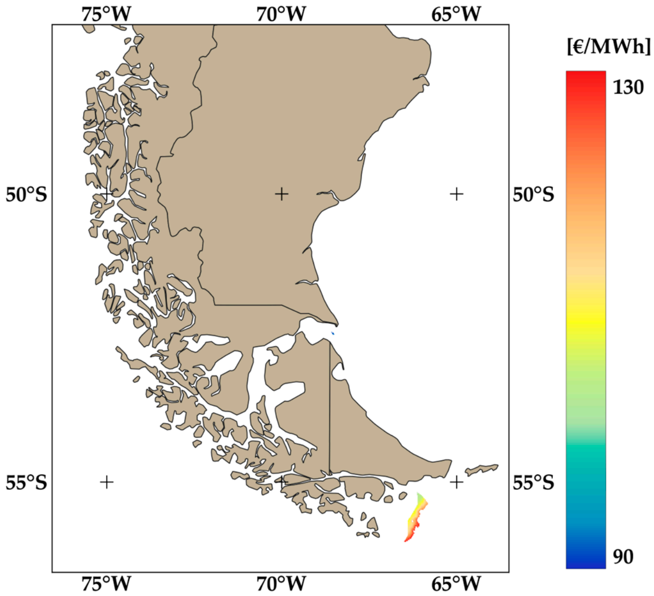

Figure 17. Chile south coast LCOE (<130 €/MWh) map.

The other zones with LCOE values less than 130 €/MWh are distributed in different locations along its extensive coast, with those located in the middle zone being shown in Figure 18. The areas shown on the map from south to north are located in the Los Lagos region, Biobío region, Maule region, O'Higgins region, and Valparaiso region, the latter two close to the Santiago Metropolitan region, which is the most populated region in Chile. Furthermore, there is also a small area that does not appear in these two maps, near Antofagasta.

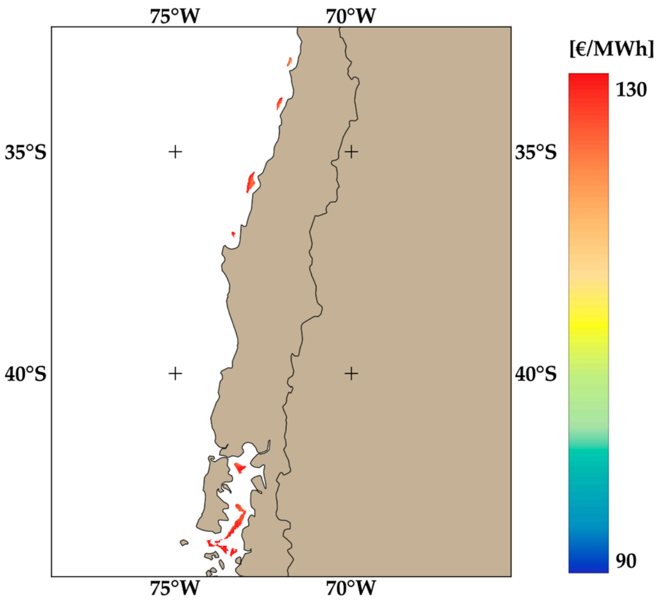

Figure 18. Chile middle coast LCOE (<130 €/MWh) map.

4. Conclusions

This study presents a world map representing the LCOE of FOW. It shows the actual potential of the technology in different regions across the planet, highlighting those where it is more suitable. This represents the next step in the evaluation of the potential of FOW compared to only assessing the wind resources, as variable cost factors have been considered depending on the bathymetry, ocean conditions, distance to shore, and distance to port. In addition, the AEP is estimated based on the average wind speed at the hub height of the exemplar wind turbine, associated capacity factors, and a series of losses in its production and transmission to shore. Furthermore, it allows for comparing several territories by drawing up rankings and taking into account not only the LCOE of their feasible areas but also their electricity production needs.

The first analysis of the results shows that within the range of values obtained, there are many areas that exceed the limits for economically feasible performance. However, it also reveals many areas where this technology is at least interesting.

The sensitivity analyses in Sections 3.2 and 3.3 reveal the impacts on the LCOE. As in other studies, the largest effect comes from the variance of the capacity factor, which has a huge effect on power output, followed by the discount rate (which has a direct impact on the LCOE function) and the cost reductions of the wind turbine and substructure. The 25% variation in each of these values in favour of LCOE reduction shows a relative decrease of 20.00%, 14.77%, 6.86%, and 4.41%, respectively. The subsequent greatest decreases in descending order come from the variation in OPEX, electrical costs, distance to shore, average significant wave height, installation costs, and mooring system costs, with relative decreases ranging from 1.57% to 4.32%.

The lowest values of LCOE obtained are analysed with the ranking of territories. The selection of territories to be analysed is described in Section 3.4, resulting in 56 territories that meet the required criteria. The analysis focuses on potential areas (areas with LCOE <130 €/MWh), the LCOE mean for 20% of the 2022 electricity production of the territory with FOW energy, and the LCOE mean of the best area to place the evaluated FOWF. A top 10 areas are determined for each factor. Next, a ranking of the 10 best territories is presented with a score out of 100, depending exclusively on the values obtained from these three factors. This process helps to assess the most potential areas and territories that have the best technical–economic conditions to apply this technology in terms of LCOE. According to the results, South America contains the best areas to exploit FOW energy, sweeping the ranking with the 4 best countries and 5 countries in the top 10. The rest of the countries in the top 10—Canada, New Zealand, Egypt, Vietnam, and the United Kingdom—are fairly dispersed around the world.

Further work can introduce new parameters or improve those used for the calculations, such as soil conditions, which determine the anchor type selection and therefore affect the costs, or the onshore substation locations, to consider them as distances for electrical costs instead of the distance to the nearest point of the coast. Furthermore, new data from future projects can be easily added to the regression models in order to achieve more accurate and updated results and better statistical quality. Moreover, a further step can be taken in the analysis of the resulting territories with the more potential by adding other differential aspects such as restrictions that have not been considered in this study, favourable political incentives, competitiveness in the country's market, or environmental impacts.

Author Contributions: Conceptualisation, S.V.L. and J.I.R.; methodology, S.V.L., J.I.R. and J.L.D.-G.; software, S.V.L. and J.I.R.; investigation, S.V.L. and J.I.R.; data curation, S.V.L. and J.I.R.; writing—original draft preparation, S.V.L.; writing—review and editing, J.I.R. and J.L.D.-G.; visualisation, S.V.L.; supervision, J.L.D.-G. All authors have read and agreed to the published version of the manuscript.

Funding: This research received no external funding.

Institutional Review Board Statement: Not applicable.

Informed Consent Statement: Not applicable.

Data Availability Statement: The data that support the findings of this study are available on request from the corresponding author.

Conflicts of Interest: The authors declare no conflicts of interest.

Appendix A

Table A1. Details of each territory with LCOE < 130 €/MWh within their EEZ.

Position	Territory	Score	Potential Area (km^2)	LCOE Mean for the Set Electricity Production (€/MWh)	Power Needed for the Set Production (MW)	Minimum LCOE for the FOWF (€/MWh)
1	Argentina	95.04	216,234	94.25	5322	92.41
2	Peru	68.84	17,852	90.79	2032	89.8
3	Colombia	67.56	11,668	92.34	2866	89.15
4	Venezuela	65.60	16,688	94.05	3402	91.07
5	Canada	62.89	164,356	110.75	26,523	108.48
6	New Zealand	50.89	20,953	103.32	1733	102.09
7	Egypt	48.99	3470	112.77	8400	95.09
8	Vietnam	47.56	8304	107.50	10,010	100.91
9	United Kingdom	43.54	52,176	112.15	12,542	109.86
10	Chile	41.53	4203	110.39	3416	105.02
11	Sweden	37.88	48,953	113.99	732	114.38
12	Taiwan	37.32	12,448	111.88	12,208	110.13
13	Ireland	33.46	14,190	113.93	1493	113.38
14	Denmark	32.99	9216	113.69	1462	113.21
15	Costa Rica	32.16	1192	113.15	573	113.11
16	Norway	31.69	26,438	117.23	6905	115.29
17	Estonia	29.53	11,699	115.80	304	116.1
18	Australia	28.93	14,494	119.57	11,311	114.79
19	Finland	28.91	12,570	116.73	3157	116.34
20	Russia	28.39	32,255	121.67	51,305	117.07
21	Brazil	26.81	1993	129.65	31,908	108.47
22	China	26.48	6853	141.23	406,157	102.15
23	Greece	26.29	9782	118.27	2307	117.76
24	Poland	25.06	8901	119.75	7651	118.01
25	United States	24.64	21,989	127.90	195,283	115.43
26	Iceland	22.76	8957	120.61	911	120.02
27	Morocco	22.28	3128	120.14	1891	119.86
28	Dominican Republic	22.12	224	118.76	777	120.43
29	Mexico	18.80	1769	127.93	16,251	118.42
30	Philippines	18.78	967	124.98	5025	120.22
31	Türkiye	18.70	1036	129.78	15,472	117.21
32	France	17.87	3471	127.36	25,890	120.12
33	Japan	17.40	5245	128.57	46,545	120.16
34	Sri Lanka	17.11	899	127.08	7872	120.7
35	India	11.17	1322	147.74	90,371	113.95
36	Cuba	10.04	77	130.62	957	126.11
37	Spain	7.51	231	135.05	12,605	126.07

Appendix B

Table A2. Details of each territory with LCOE < 130 within their EEZ that do not pass all the restrictions to be considered for the ranking.

Position *	Territory	Score	Potential Area (km^2)	LCOE Mean for the Set Electricity Production (€/MWh)	Power Needed for the Set Production (MW)	Minimum LCOE for the FOWF (€/MWh)
2	Falkland Islands	69.25	92,492	97.47	11	97.76
7	Aruba	58.20	2966	94.76	36	96.48
8	Alaska	53.49	42,507	102.78	272	103.25
10	Madagascar	49.38	2667	101.05	89	102.12
14	Namibia	41.84	11,850	107.46	65	107.89
16	Mauritania	41.40	12,642	107.29	85	108.62
17	Yemen	40.61	558	106.17	160	108.15
18	Eritrea	38.19	1511	108.64	36	109.4
21	Saint Pierre and Miquelon	37.32	3903	109.63	12	110.13
22	Nicaragua	36.69	3999	110.05	215	110.57
24	Western Sahara	33.05	31,695	No data	No data	94.88
29	Latvia	29.27	9315	115.39	255	116.25
32	Somalia	28.83	16,878	115.92	18	117.69
35	Cabo Verde	26.76	95	113.65	35	118.58
41	Faroe Islands	22.35	1150	118.39	26	120.58
42	Lithuania	22.31	1242	119.43	175	119.97
45	Fiji	21.96	695	119.06	52	120.49
46	Turks and Caicos	20.52	1082	120.32	17	121.35
53	Papua New Guinea	14.16	190	123.86	234	125.94

* The position that would be achieved if restrictions had not been applied.

References

1. Sustainable Development Goals. 13 Climate Action. Available online: https://www.un.org/sustainabledevelopment/climate-change/ (accessed on 7 August 2023).
2. Hutchinson, M.; Zhao, F. *Global Wind Report 2023*; The Global Wind Energy Council: Brussels, Belgium, 2023.
3. Wind Europe. Wind Energy Today. Available online: https://windeurope.org/about-wind/wind-energy-today/ (accessed on 7 August 2023).
4. Ferčák, O.; Bossuyt, J.; Ali, N.; Cal, R.B. Decoupling Wind–Wave–Wake Interactions in a Fixed-Bottom Offshore Wind Turbine. *Appl. Energy* **2022**, *309*, 118358. [CrossRef]
5. Lerch, M. Technical-Economic Analysis, Modeling and Optimization of Floating Offshore Wind Farms. Ph.D. Thesis, Polytechnic University of Catalonia, Barcelona, Spain, 2020.
6. Brussa, G.; Grosso, M.; Rigamonti, L. Life Cycle Assessment of a Floating Offshore Wind Farm in Italy. *Sustain. Prod. Consum.* **2023**, *39*, 134–144. [CrossRef]
7. Martinez, A.; Iglesias, G. Multi-Parameter Analysis and Mapping of the Levelised Cost of Energy from Floating Offshore Wind in the Mediterranean Sea. *Energy Convers. Manag.* **2021**, *243*, 114416. [CrossRef]
8. Martinez, A.; Iglesias, G. Wave Exploitability Index and Wave Resource Classification. *Renew. Sustain. Energy Rev.* **2020**, *134*, 110393. [CrossRef]
9. Khojasteh, D.; Shamsipour, A.; Huang, L.; Tavakoli, S.; Haghani, M.; Flocard, F.; Farzadkhoo, M.; Iglesias, G.; Hemer, M.; Lewis, M.; et al. A Large-Scale Review of Wave and Tidal Energy Research over the Last 20 Years. *Ocean. Eng.* **2023**, *282*, 114995. [CrossRef]
10. El Hammoumi, A.; Chtita, S.; Motahhir, S.; El Ghzizal, A. Solar PV Energy: From Material to Use, and the Most Commonly Used Techniques to Maximize the Power Output of PV Systems: A Focus on Solar Trackers and Floating Solar Panels. *Energy Rep.* **2022**, *8*, 11992–12010. [CrossRef]
11. Shen, W.; Chen, X.; Qiu, J.; Hayward, J.A.; Sayeef, S.; Osman, P.; Meng, K.; Dong, Z.Y. A Comprehensive Review of Variable Renewable Energy Levelized Cost of Electricity. *Renew. Sustain. Energy Rev.* **2020**, *133*, 110301. [CrossRef]
12. Q FWE Analyses Team. *Global Floating Wind Market and Forecast Report*; Quest Floating Wind Energy: Sugar Land, TX, USA, 2021.
13. Díaz, H.; Guedes Soares, C. An Integrated GIS Approach for Site Selection of Floating Offshore Wind Farms in the Atlantic Continental European Coastline. *Renew. Sustain. Energy Rev.* **2020**, *134*, 110328. [CrossRef]

14. Castro-Santos, L.; Filgueira-Vizoso, A.; Carral-Couce, L.; Formoso, J.Á.F. Economic Feasibility of Floating Offshore Wind Farms. *Energy* **2016**, *112*, 868–882. [CrossRef]
15. Martinez, A.; Iglesias, G. Mapping of the Levelised Cost of Energy for Floating Offshore Wind in the European Atlantic. *Renew. Sustain. Energy Rev.* **2022**, *154*, 111889. [CrossRef]
16. Christoforaki, M.; Tsoutsos, T. Sustainable Siting of an Offshore Wind Park a Case in Chania, Crete. *Renew. Energy* **2017**, *109*, 624–633. [CrossRef]
17. Caglayan, D.G.; Ryberg, D.S.; Heinrichs, H.; Linßen, J.; Stolten, D.; Robinius, M. The Techno-Economic Potential of Offshore Wind Energy with Optimized Future Turbine Designs in Europe. *Appl. Energy* **2019**, *255*, 113794. [CrossRef]
18. Schallenberg-Rodríguez, J.; García Montesdeoca, N. Spatial Planning to Estimate the Offshore Wind Energy Potential in Coastal Regions and Islands. Practical Case: The Canary Islands. *Energy* **2018**, *143*, 91–103. [CrossRef]
19. Lerch, M.; De-Prada-Gil, M.; Molins, C.; Benveniste, G. Sensitivity Analysis on the Levelized Cost of Energy for Floating Offshore Wind Farms. *Sustain. Energy Technol. Assess.* **2018**, *30*, 77–90. [CrossRef]
20. Ohunakin, O.S.; Matthew, O.J.; Adaramola, M.S.; Atiba, O.E.; Adelekan, D.S.; Aluko, O.O.; Henry, E.U.; Ezekiel, V.U. Techno-Economic Assessment of Offshore Wind Energy Potential at Selected Sites in the Gulf of Guinea. *Energy Convers. Manag.* **2023**, *288*, 117110. [CrossRef]
21. Bosch, J.; Staffell, I.; Hawkes, A.D. Global Levelised Cost of Electricity from Offshore Wind. *Energy* **2019**, *189*, 116357. [CrossRef]
22. Gaertner, E.; Rinker, J.; Sethuraman, L.; Anderson, B.; Zahle, F.; Barter, G. *IEA Wind TCP Task 37: Definition of the IEA 15 MW Offshore Reference Wind Turbine*; Technical Report; NREL/TP-5000-75698 March 2020; National Renewable Energy Laboratory: Denver, CO, USA, 2020.
23. Benveniste, G.; De-Prada, M.; Lerch, M.; Matha, D.; Norbeck, J.A.; Berthelsen, P.A.; Vita, L.; Ugwu, J.; Proskovics, R. Deliverable 2.6 Economical, Technical and Environmental Evaluation of Phase I; LIFES50plus. 2018. Available online: https://www.sintef.no/globalassets/project/industry-meets-science2/24-oktober-2018/berthelsen_l50pindustrymeetssciencepdf.pdf (accessed on 26 August 2024).
24. Myhr, A.; Bjerkseter, C.; Ågotnes, A.; Nygaard, T.A. Levelised Cost of Energy for Offshore Floating Wind Turbines in a Life Cycle Perspective. *Renew. Energy* **2014**, *66*, 714–728. [CrossRef]
25. GEBCO Compilation Group. GEBCO 2022 Grid. Available online: https://www.gebco.net/ (accessed on 3 July 2023).
26. E.U. Copernicus Marine Service Information (CMEMS). Marine Data Store (MDS). Global Ocean Waves Reanalysis. Available online: https://data.marine.copernicus.eu/product/GLOBAL_MULTIYEAR_WAV_001_032/services (accessed on 25 January 2023).
27. Technical University of Denmark; World Bank Group; Global Wind Atlas; Technical University of Denmark: Copenhagen, Denmark, 2023. Available online: https://globalwindatlas.info/en (accessed on 25 January 2023).
28. Flanders Marine Institute. Maritime Boundaries Geodatabase: Maritime Boundaries and Exclusive Economic Zones (200NM), Version 11. 2019. Available online: https://www.marineregions.org/ (accessed on 25 January 2023).
29. Maritime Safety Information. World Port Index. Available online: https://msi.nga.mil/Publications/WPI (accessed on 30 January 2024).
30. AmeriGEOSS. Global Ports. Available online: https://geonode.wfp.org/geoserver/wfs?format_options=charset:UTF-8&typename=geonode:wld_trs_ports_wfp&outputFormat=SHAPE-ZIP&version=1.0.0&service=WFS&request=GetFeature (accessed on 7 August 2023).
31. COREWIND. Cost Reduction and Increase Performance of Floating Wind Technology. 2021. Available online: https://corewind.eu/ (accessed on 25 January 2023).
32. James, R.; Costa Ros, M. *Floating Offshore Wind: Market and Technology Review*; The Carbon Trust: London, UK, 2015; Available online: https://ctprodstorageaccountp.blob.core.windows.net/prod-drupal-files/documents/resource/public/Floating%20Offshore%20Wind%20Market%20Technology%20Review%20-%20REPORT.pdf (accessed on 25 January 2023).
33. Heidari, S. Economic Modelling of Floating Offshore Wind Power, Mälardalen University, School of Business, Society and Engineering, Industrial Economics and Organisation, Master Thesis. 2017. Available online: https://mdh.diva-portal.org/smash/record.jsf?pid=diva2:1128321&dswid=-7514 (accessed on 25 January 2023).
34. Maness, M.M.B.S.A. *NREL Offshore Balance-of-System Model*; National Renewable Energy Laboratory: Denver, CO, USA, 2017.
35. Metych, M. Exclusive Economic Zone. Available online: https://www.britannica.com/topic/exclusive-economic-zone (accessed on 7 August 2023).
36. *IEC 61400-1*; Wind Energy Generation Systems-Part 1: Design Requirements, Volume 4. International Electrotechnical Commission: Geneva, Switzerland, 2019.
37. Campanile, A.; Piscopo, V.; Scamardella, A. Mooring Design and Selection for Floating Offshore Wind Turbines on Intermediate and Deep Water Depths. *Ocean. Eng.* **2018**, *148*, 349–360. [CrossRef]
38. Ojo, A.; Collu, M.; Coraddu, A. Multidisciplinary Design Analysis and Optimization of Floating Offshore Wind Turbine Substructures: A Review. *Ocean. Eng.* **2022**, *266*, 112727. [CrossRef]
39. Ng, C.; Ran, L. Introduction to Offshore Wind Energy. In *Offshore Wind Farms: Technologies, Design and Operation*; Woodhead Publishing: London, UK, 2016; pp. 3–8. ISBN 978-0-08-100779-2.
40. Maienza, C.; Avossa, A.M.; Ricciardelli, F.; Coiro, D.; Troise, G.; Georgakis, C.T. A Life Cycle Cost Model for Floating Offshore Wind Farms. *Appl. Energy* **2020**, *266*, 114716. [CrossRef]

41. Benveniste, G.; Lerch, M.; De-Prada, M.; Kretschmer, M.; Berqué, J.; López, A.; Pérez, G. Deliverable 2.2. LCOE Tool. Description, Technical and Environmental Impact Evaluation Procedure; LIFES50plus. 2018. Available online: https://www.sintef.no/globalassets/project/industry-meets-science2/24-oktober-2018/berthelsen_l50pindustrymeetssciencepdf.pdf (accessed on 26 August 2024).
42. Frost, J. How to Interpret Regression Analysis Results: P-Values and Coefficients. Available online: https://statisticsbyjim.com/regression/interpret-coefficients-p-values-regression/ (accessed on 7 August 2023).
43. Prasetya, D.A.; Nguyen, P.T.; Faizullin, R.; Iswanto, I.; Armay, E.F. Resolving the Shortest Path Problem Using the Haversine Algorithm. *J. Crit. Rev.* **2020**, *7*, 62–64.
44. Sourianos, E.; Kyriakou, K.; Hatiris, G.A. GIS-Based Spatial Decision Support System for the Optimum Siting of Offshore Windfarms. *Eur. Water* **2017**, *58*, 337–343.
45. UNEP-WCMC and IUCN (2023), Protected Planet. The World Database on Protected Areas (WDPA) and World Database on Other Effective Area-Based Conservation Measures (WD-OECM) [Online], January 2023, Cambridge, UK: UNEP-WCMC and IUCN. Available online: https://www.protectedplanet.net/en (accessed on 25 January 2023).
46. Ember With Major Processing by Our World in Data, "Yearly Electricity Data". Available online: https://ourworldindata.org/grapher/electricity-generation (accessed on 19 December 2023).
47. Enevoldsen, P.; Jacobson, M.Z. Data Investigation of Installed and Output Power Densities of Onshore and Offshore Wind Turbines Worldwide. *Energy Sustain. Dev.* **2021**, *60*, 40–51. [CrossRef]
48. The World Bank. Global Offshore Wind Technical Potential. Available online: https://datacatalog.worldbank.org/search/dataset/0037787 (accessed on 15 May 2024).
49. Biancucci, M.; Labriola, C. Propuesta Para Generacion Combinada Eolico-Mareomotriz En La Patagonia. *Av. En. Energ. Renov. Medio Ambiente* **2007**, *11*, 7–14. Available online: http://sedici.unlp.edu.ar/handle/10915/92909 (accessed on 26 August 2024).
50. IEA. Latin America's Hydrogen Opportunity: From National Strategies to Regional Cooperation. IEA: Paris, France, 2020; Available online: https://www.iea.org/commentaries/latin-america-s-hydrogen-opportunity-from-national-strategies-to-regional-cooperation (accessed on 9 May 2024).
51. Costoya, X.; deCastro, M.; Santos, F.; Sousa, M.C.; Gómez-Gesteira, M. Projections of Wind Energy Resources in the Caribbean for the 21st Century. *Energy* **2019**, *178*, 356–367. [CrossRef]
52. Bethel, B.J. Joint Offshore Wind and Wave Energy Resources in the Caribbean Sea. *J. Mar. Sci. Appl.* **2021**, *20*, 660–669. [CrossRef]
53. Rueda-Bayona, J.G.; Guzmán, A.; Eras, J.J.C.; Silva-Casarín, R.; Bastidas-Arteaga, E.; Horrillo-Caraballo, J. Renewables Energies in Colombia and the Opportunity for the Offshore Wind Technology. *J. Clean. Prod.* **2019**, *220*, 529–543. [CrossRef]
54. Global Wind Energy Council. *Floating Offshore Wind—A Global Opportunity*; The Global Wind Energy Council: Brussels, Belgium, 2022.
55. Dong, C.; Huang, G.; Cheng, G. Offshore Wind Can Power Canada. *Energy* **2021**, *236*, 121422. [CrossRef]
56. Zheng, C.; Li, C.; Xu, J. Micro-Scale Classification of Offshore Wind Energy Resource—A Case Study of the New Zealand. *J. Clean. Prod.* **2019**, *226*, 133–141. [CrossRef]
57. Mahdy, M.; Bahaj, A.S. Multi Criteria Decision Analysis for Offshore Wind Energy Potential in Egypt. *Renew. Energy* **2018**, *118*, 278–289. [CrossRef]
58. Cavazzi, S.; Dutton, A.G. An Offshore Wind Energy Geographic Information System (OWE-GIS) for Assessment of the UK's Offshore Wind Energy Potential. *Renew. Energy* **2016**, *87*, 212–228. [CrossRef]
59. Mattar, C.; Cabello-Españon, F.; Alonso-de-Linaje, N.G. Towards a Future Scenario for Offshore Wind Energy in Chile: Breaking the Paradigm. *Sustainability* **2021**, *13*, 7013. [CrossRef]